Molecular Crystals and Liquid Crystals

ISSN: 1542-1406 (Print) 1563-5287 (Online) Journal homepage: http://www.tandfonline.com/loi/gmcl20

Synthesis, Crystal Structure, and Spectroscopic Properties of (Z)-4-(2-Methoxybenzylidene)-1-methyl-2-phenyl-1H-imidazol-5(4H)-one

Jiun-Wei Hu & Kew-Yu Chen

To cite this article: Jiun-Wei Hu & Kew-Yu Chen (2015) Synthesis, Crystal Structure, and Spectroscopic Properties of (Z)-4-(2-Methoxybenzylidene)-1-methyl-2-phenyl-1H-imidazol-5(4H)-one, Molecular Crystals and Liquid Crystals, 623:1, 379-387, DOI: 10.1080/15421406.2015.1036507

To link to this article: http://dx.doi.org/10.1080/15421406.2015.1036507

Published online: 21 Dec 2015.

Mol. Cryst. Liq. Cryst., Vol. 623: pp. 379–387, 2015

ISSN: 1542-1406 print/1563-5287 online
DOI: 10.1080/15421406.2015.1036507

Synthesis, Crystal Structure, and Spectroscopic Properties of (*Z*)-4-(2-Methoxybenzylidene)-1-methyl-2-phenyl-1*H*-imidazol-5(4*H*)-one

JIUN-WEI HU AND KEW-YU CHEN*

Department of Chemical Engineering, Feng Chia University, Taichung, Taiwan, ROC

*The title compound, (Z)-4-(2-methoxybenzylidene)-1-methyl-2-phenyl-1H-imidazol-5(4H)-one (**1**), was synthesized and characterized. Compound **1** possesses two weak intramolecular C–H···O and C–H···N hydrogen bonds, which generate S(5) and S(6) rings, respectively. Intermolecular π–π stacking between the imidazolone ring and its adjacent one is observed in the crystal structure, which links a pair of molecules into a cyclic centrosymmetric dimer. Furthermore, two different C–H···π interactions lead to the formation of columns along the [100] direction that are connected to one another via intermolecular C–H···O hydrogen bonds, so linking the molecules into a continuous three-dimensional framework. Its spectroscopic properties and complementary density functional theory calculations are also reported.*

Keywords Density functional theory; imidazolone; X-ray diffraction

1. Introduction

Imidazolones and their related derivatives are a class of important heterocyclic compounds and show a variety of biological and pharmaceutical properties such as anticancer, antiinflammatory, and angiotensin II receptor antagonistic activity [1–12]. Additionally, many imidazolone derivatives have been successfully isolated from the incubation mixture of 3-deoxyglucosone (3-DG) and an arginine derivative as novel advanced glycation end products [13,14]. In an effort to expand the scope of imidazolone-based chromophores available for designing systems for biologically active molecules and fluorescent dyes, the present research reports the synthesis of a new imidazolone derivative (**1**) as well as its X-ray structure, photophysical properties, and complementary density functional theory (DFT) calculations. The results offer the potential to synthesize imidazolone derivatives with extended molecular architectures and optical properties.

*Address correspondence to Kew-Yu Chen, Department of Chemical Engineering, Feng Chia University, Taichung 40724, Taiwan, ROC. E-mail: kyuchen@fcu.edu.tw

Color versions of one or more of the figures in the article can be found online at www.tandfonline.com/gmcl.

2. Experimental

2.1. Chemicals and Instruments

The starting materials such as 2-methoxybenzaldehyde (**4**), 2-benzamidoacetic acid (**3**), sodium acetate, acetic anhydride, methylamine, and potassium carbonate were purchased from Merck, ACROS and Sigma–Aldrich. Column chromatography was performed using silica gel Merck Kieselgel *si* 60 (40–63 mesh).

^{1}H and ^{13}C NMR spectra were recorded in $CDCl_3$ on a Bruker 400 MHz. Mass spectra were recorded on a VG70-250S mass spectrometer. The absorption and emission spectra were measured using a Jasco V-570 UV–Vis spectrophotometer and a Hitachi F-4500 fluorescence spectrophotometer, respectively. The single-crystal X-ray diffraction data were collected on a Bruker Smart 1000CCD area-detector diffractometer.

2.2. Synthesis and Characterization

2.2a Synthesis of ***1.*** (*Z*)-4-(2-methoxybenzylidene)-2-phenyloxazol-5(4*H*)-one (**2**, 1.0 g, 3.6 mmol) was added to potassium carbonate (0.5 g, 3.6 mmol) in a 50-mL round-bottom flask, to which 20 mL ethanol (95%) and 1.0 mL methylamine (40% aqueous) were then added. The reaction mixture was refluxed for 4 hr. After cooling, the mixture was neutralized with 10% HCl and extracted with CH_2Cl_2 (3 × 25 mL). After solvent was removed, the crude product was purified by silica gel column chromatography with eluent ethyl acetate/*n*-hexane (1/2) to afford **1**. Yield: 85%. m.p.: 176∼177° C. Anal. Calcd. (%) for $C_{18}H_{16}N_2O_2$: C 73.95; H 5.52; N 9.58. Found (%): C, 73.69; H, 5.56; N 9.80. ^{1}H NMR (400 MHz, $CDCl_3$, in ppm) δ 8.92 (*d*, $J = 7.6$ Hz, 1H), 7.85 ∼ 7.83 (m, 3H), 7.56 ∼ 7.52 (m, 3H), 7.37 (*t*, $J = 8.4$ Hz, 1H), 7.04 (*t*, $J = 7.6$ Hz, 1H), 6.91 (*d*, $J = 8.3$ Hz, 1H), 3.90 (s, 3H), 3.37 (s, 3H); ^{13}C NMR (100 MHz, $CDCl_3$, in ppm) 171.7, 161.8, 159.3, 138.4, 133.3, 131.9, 131.3, 129.5, 128.7, 128.6, 123.4, 122.9, 120.9, 110.5, 55.5, 29.0; MS (EI, 70eV): *m/z* (relative intensity) 292 (M^+, 100); HRMS calcd. for $C_{18}H_{16}N_2O_2$ 292.1212, found 292.1219. Orange needle-shaped crystals suitable for the crystallographic studies reported here were isolated over a period of six weeks by slow evaporation from a dichloromethane solution.

2.2b Crystal Structural Determination. A single crystal of the title compound with dimensions of 0.36 mm× 0.10 mm× 0.10 mm was selected. The lattice constants and diffraction intensities were measured with a Bruker Smart 1000CCD area detector radiation (λ = 0.71073 Å) at 150.0(1) K. An ω-2θ scan mode was used for data collection in the range of $2.14 \leqq \theta \leqq 25.03°$. A total of 20213 reflections were collected and 2545 were independent ($R_{int} = 0.0232$), of which 1435 were considered to be observed with $I > 2\sigma(I)$ and used in the succeeding refinement. The structure was solved by direct methods with SHELXS-97 [15] and refined on F^2 by full-matrix least-squares procedure with Bruker SHELXL-97 packing [16]. All non-hydrogen atoms were refined with anisotropic thermal parameters. The hydrogen atoms refined with riding model position parameters isotropically were located from difference Fourier map and added theoretically. At the final cycle of refinement, $R = 0.0299$ and $wR = 0.0559$ ($w = 1/[\sigma^2(F_o^2) + (0.0239P)^2 + 0.0000P]$, where $P = (F_o^2 + 2F_c^2)/3$). $S = 0.752$, $(\Delta/\sigma)_{max} = 0.000$, $(\Delta/\rho)_{max} = 0.133$ and $(\Delta/\rho)_{min} = -0.145$ e/Å^3. Crystallographic data for compound **1** have been deposited with the Cambridge Crystallographic Data Center as supplementary publication number CCDC 1040178. Copies of these information can be obtained free of charge from the Director, CCDC, 12 Union Road, Cambridge CB2 1EZ, UK (fax: +44 1223 336 033; e-mail: deposit@ccdc.cam.ac.uk).

2.3. Computational Methods

The Gaussian 03 program was used to perform the ab initio calculation on the molecular structure [17]. Geometry optimization for compound **1** was carried out with the 6-31G** basis set to the B3LYP functional. After obtaining the converged geometries, the TD-B3LYP/6-31G** was used to calculate the vertical excitation energy, and the emission energy was obtained from TDDFT/B3LYP/6-31G** calculations performed on S_1 optimized geometries.

3. Results and Discussion

Scheme 1 shows the synthetic route and the chemical structure of **1**. The synthesis started from a condensation reaction of 2-methoxybenzaldehyde (**4**) and 2-benzamidoacetic acid (**3**) in the presence of sodium acetate, giving an oxazolone derivative (**2**). Subsequent reaction of **2** with methylamine afforded the imidazolone compound **1**. The structure of **1** can be verified by the presence of two singlet signals at δ 3.3 and 3.9 ppm in the ^{1}H NMR spectrum, which are attributed to the signals of two chemically different methyl protons at the N(1) and O(2) atoms, respectively. Detailed synthetic procedures and product characterization are provided in the Experimental Section. To confirm its structure, a single crystal of **1** was obtained from a dichloromethane solution, and the molecular structure was determined by X-ray diffraction analysis. In addition, its X-ray structure is compared with that of **2** [18].

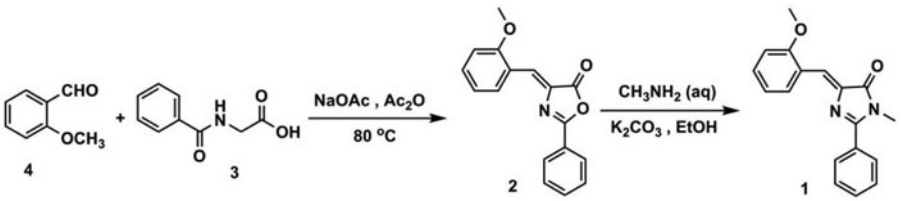

Scheme 1. The synthetic route for 1.

Compound **1** crystallizes in the monoclinic space group $P2_1/c$, with $a = 7.1121(6)$, $b = 11.2091(11)$, $c = 18.2146(18)$ Å, $\alpha = 90°$, $\beta = 97.377(2)°$, ($\gamma = 90°$, and Z = 4, whereas compound 2 [18] crystallizes in the triclinic space group P-1, with a = 8.8073(6), b = 9.6140(6), c = 9.8272(6) Å, ($\alpha = 66.503(4)°$,$\beta = 67.(= 67.248(4)°$, ($\gamma = 71.734(4)°$, and Z = 2. Both compounds 1 and 2 possess normal geometric parameters (Table 1) and adopt a *Z* configuration about the central olefinic bond. The dihedral angle between the mean planes of the benzylidene ring and the imidazolone ring in **1** is 12.4(2)º, while that of the imidazolone ring and the phenyl ring is as large as 39.5(2)°. This twisted conformation is most probably caused by the repulsion (Fig. 1) of the hydrogen atoms H(4A) and H(14). In contrast, the phenyl ring is almost coplanar with the plane of the oxazolone ring in **2** (Fig. 2), making a dihedral angle of only 2.0(1)º [18]. Moreover, both **1** and **2** possess two weak intramolecular C–H···O and C–H···N hydrogen bonds (Table 2), which generate S(5) and S(6) rings, respectively. These intramolecular hydrogen bonds further stabilize both structures and make the benzylidene ring roughly coplanar with respect to the imidazolone (oxazolone) ring.

Figure 3 shows the molecular packing of **1** in the crystal unit cell. The crystal structure is stabilized by two different intermolecular C–H···O hydrogen bonds (Table 2). Furthermore, intermolecular π–π stacking (*Cg*1–*Cg*1, Cg1 is the centroid of the imidazolone

Table 1. Comparison of the experimental and optimized geometric parameters of **1** (Å and °)

	X-ray	DFT
Bond lengths (Å)		
O(1)-C(2)	1.2253 (16)	1.2210
O(2)-C(7)	1.3624 (17)	1.3623
N(1)-C(1)	1.3954 (17)	1.3966
N(1)-C(2)	1.3856 (19)	1.4084
N(1)-C(4)	1.4523 (17)	1.4522
C(3)-C(5)	1.3472 (19)	1.3611
C(5)-C(6)	1.454 (2)	1.449
C(1)-C(13)	1.4683 (18)	1.471
Bond angles (°)		
C(7)-O(2)-C(12)	117.83 (12)	119.03
C(1)-N(1)-C(1)	107.60 (12)	107.54
C(2)-N(1)-C(4)	122.14 (12)	121.10
C(1)-N(2)-C(3)	105.87 (12)	106.67
N(2)-C(1)-N(1)	114.02 (12)	113.54
O(1)-C(2)-N(1)	125.21 (12)	125.18
Torsion angles (°)		
C(5)-C(6)-C(7)-O(2)	–1.01 (13)	–0.33
N(2)-C(3)-C(5)-C(6)	0.13 (12)	0.43
O(1)-C(2)-N(1)-C(1)	177.05 (12)	177.67
N(2)-C(1)-C(13)-C(14)	140.18 (12)	143.66

ring) between the imidazolone ring and its adjacent one is also observed in the crystal structure, which links a pair of molecules into a cyclic centrosymmetric dimer. Pertinent measurements for these $\pi\cdots\pi$ interactions are: centroid–centroid distances of 3.6602(9) (green-dashed line in Fig. 3, symmetry code: *–X*, 2*–Y*, *–Z*) and 4.1026(9) Å (blue-dashed line in Fig. 3, symmetry code: 1*–X*, 2*–Y*, *–Z*). The crystal packing is further stabilized by two intermolecular C–H$\cdots\pi$ interactions; one between the H(4A) atom of methyl group and the phenyl ring (Cg2 is the centroid of C6–C11 ring) of a neighboring molecule (black-dashed line in Fig. 3, symmetry code: *–X*, 2*–Y*, *–Z*), a second between the H(4C) atom and the same phenyl ring, respectively (red-dashed line in Fig. 3, symmetry code: 1–X, 2–Y, –Z). These C–H$\cdots\pi$ interactions lead to the formation of columns along the [100] direction that are connected to one another *via* intermolecular C–H$\cdots$O hydrogen bonds, so linking the molecules into a continuous three-dimensional framework.

The steady-state absorption and emission spectra of **1** in cyclohexane are shown in Fig. 4. The lowest energy absorption band of **1** appears at 392 nm, which is assigned to the π–π^* transitions (vide infra). Two higher energy absorption bands are also observed at 252 and 292 nm, respectively. As for the steady-state emission, compound **1** shows a blue emission (470 nm) with Φ_f as low as 0.002. The low fluorescence quantum yield suggests an effective radiationless transition operating in **1**, induced by conformational relaxation along torsional deformation of the two exocyclic C–C bonds, from the initially Franck-Condon state to a nonfluorescent twisted intermediate.

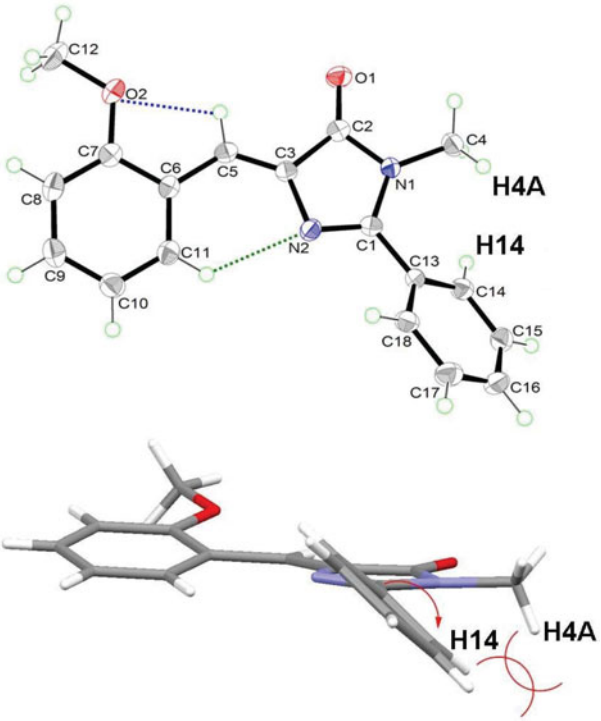

Figure 1. The X-ray crystal structures of **1** with displacement atomic ellipsoids drawn at the 50% probability level. Blue- and green-dashed lines denote the intramolecular C–H···O and C–H···N hydrogen bonds.

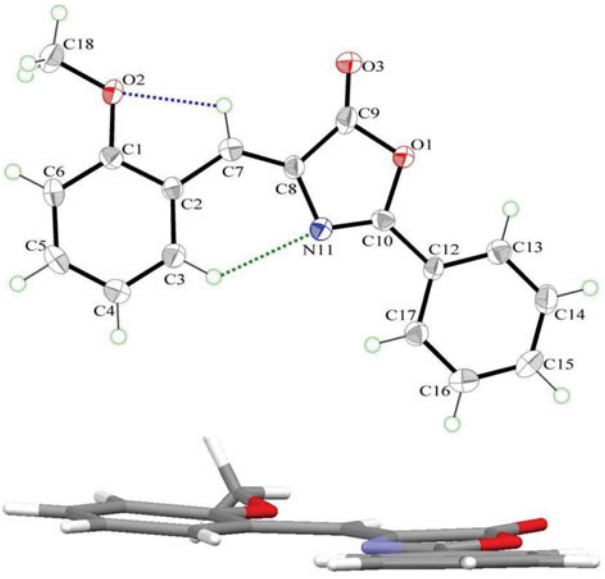

Figure 2. The X-ray crystal structures of **2** with displacement atomic ellipsoids drawn at the 50% probability level. Blue- and green-dashed lines denote the intramolecular C–H···O and C–H···N hydrogen bonds.

Table 2. Hydrogen-bond geometry (Å, º)

D–H···*Cg*	d(D–H)	d(H···*Cg*)	d(D···*Cg*)	∠DH*Cg*
C(5)–H(5)···O2	0.93	2.35	2.7205 (17)	103
C(11)–H(11)···N2	0.93	2.40	3.038 (2)	126
C(12)–H(12C)···O1[a]	0.96	2.60	3.0963 (18)	113
C(15)–H(15)···O1[b]	0.93	2.59	3.4974 (18)	167

Symmetry codes: (a) $-x+1, y+1/2, -z+1/2$; (b) $x, -y+3/2, z-1/2$.

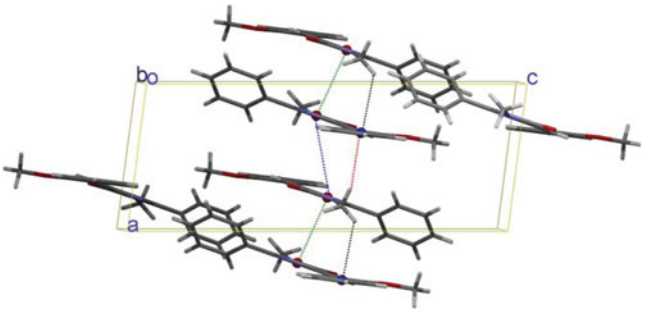

Figure 3. A packing view of **1**, viewed along the *b* axis. Black- and red-dashed lines denote the intermolecular C(4)–H(4A)···*Cg*2 and C(4)–H(4C)···*Cg*2 interactions, respectively. Green- and blue-dashed lines denote strong and weak π–π (*Cg*1–*Cg*1) interactions, respectively. *Cg*1 (red circle) and *Cg*2 (blue circle) are the centroids of the N1/C1/N2/C3/C2 and C6–C11 rings, respectively.

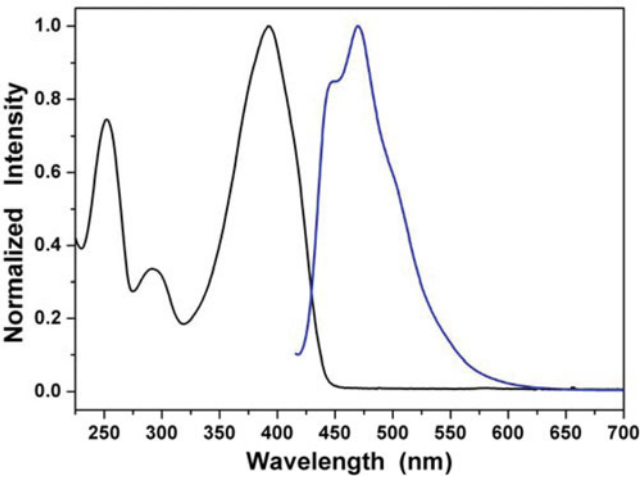

Figure 4. Normalized absorption (black line) and emission (blue line) spectra of **1** in cyclohexane solution.

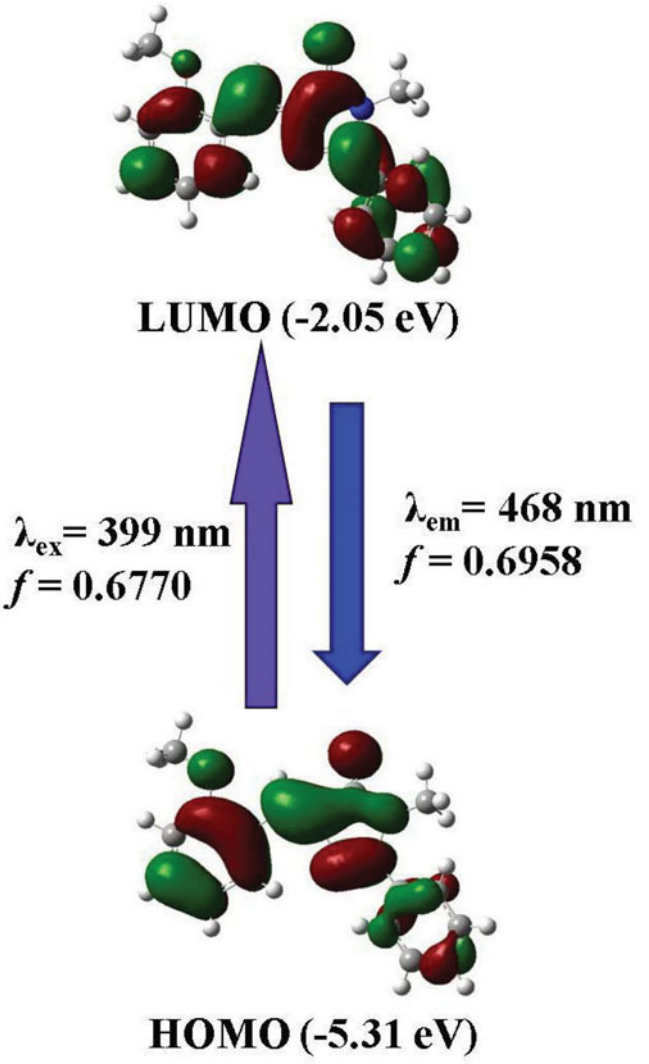

Figure 5. Computed frontier orbitals of **1**.

To gain more insight into the molecular structure and electronic properties of **1**, quantum chemical calculations were performed using DFT at the B3LYP/6-31G** level. The values of bond lengths, bond angles, and torsion angles were compared with experimental data (Table 1). There are no obvious differences between the experimental and DFT/B3LYP calculated geometric parameters. Therefore, we can conclude that basis set 6–31G** is suited in its approach to the experimental results.

Figure 5 shows the highest occupied molecular orbital (HOMO) and the lowest unoccupied molecular orbital (LUMO) of **1**. The HOMO is delocalized mainly on the benzylidene fragment and the imidazolone moiety, while the LUMO is delocalized extensively over the whole π–conjugated system from the benzylidene fragment to the imidazolone and phenyl rings. Moreover, the absorption and emission spectra of **1** were calculated by time-dependent DFT (TD-DFT) calculations (Franck–Condon principle). The calculated

excitation (fluorescence) wavelength for the $S_0 \rightarrow S_{1\text{-}}$ ($S_1 \rightarrow S_0$) transition is 399 (468) nm, which is very close to the experimental results.

4. Conclusions

An imidazolone derivative, (*Z*)-4-(2-methoxybenzylidene)-1-methyl-2-phenyl-1*H*-imidazol-5(4*H*)-one (**1**), was synthesized and characterized by single-crystal X-ray diffraction. The crystal belongs to monoclinic, space group $P2_1/c$, with $a = 7.1121(6)$, $b = 11.2091(11)$, $c = 18.2146(18)$ Å, $\alpha = 90^\circ$, $\beta = 97.377(2)^\circ$, $\gamma = 90^\circ$. Additionally, the single-crystal X-ray structure determinations described here have brought to light a number of interesting properties between **1** and **2** in the solid phase, including $\pi\cdots\pi$ stacking and intra- and intermolecular hydrogen bonding interactions. Compound **1** shows a blue emission with Φ_f as low as 0.002. The low fluorescence quantum yield suggests an effective radiationless transition operating in **1**, induced by conformational relaxation along torsional deformation of the two exocyclic C–C bonds, from the Franck-Condon state to a nonfluorescent twisted intermediate. Its molecular geometry in the ground state has also been calculated using DFT at the B3LYP/6-31G** level and compared with its crystal structure. The results show that the optimized geometry can well reproduce the crystal structure.

Acknowledgments

The project was supported by the Ministry of Science and Technology (MOST 103-2113-M-035-001) in Taiwan. The authors appreciate the Precision Instrument Support Center of Feng Chia University for providing the fabrication and measurement facilities.

References

[1] Mittelmaier, S., & Pischetsrieder, M. (2011). *Anal. Chem.*, *83*, 9660.
[2] Lopez-Clavijo, A. F., Barrow, M. P., Rabbani, N., Thornalley, P. J., & O'Connor, P. B. (2012). *Anal. Chem.*, *84*, 10568.
[3] Siamaki, A. R., Black, D. A., & Arndtsen, B. A. (2008). *J. Org. Chem.*, *73*, 1135.
[4] Kim, S. B., Suzuki, H., Sato, M., & Tao, H. (2011). *Anal. Chem.*, *83*, 8732.
[5] Amano, M., Kobayashi, N., Yabuta, M., Uchiyama, S., & Fukui, K. (2014). *Anal. Chem.*, *86*, 7536.
[6] Gomha, S. M., & Hassaneen, H. M. E. (2011). *Molecules*, *16*, 6549.
[7] El-Araby, M., Omar, A., Hassanein, H. H., El-Helby, A. H., & Abdel-Rahman, A. A. (2012). *Molecules*, *17*, 12262.
[8] Amano, M., Hasegawa, J., Kobayashi, N., Kishi, N., Nakazawa, T., Uchiyama, S., & Fukui, K. (2011). *Anal. Chem.*, *83*, 3857.
[9] Akçay, H. T., Bayrak, R., Demirbas, Ü., Koca, A., Kantekin, H., & Değirmencioğlu, I. (2013). *Dyes Pigm.*, *96*, 483.
[10] Zhang, X. H., Zhan, Y. H., Chen, D., Wang, F., & Wang, L. Y. (2012). *Dyes Pigm.*, *93*, 1408.
[11] Fang, L., He, Q., Hu, Y., & Yang, B. (2007). *Cancer Chemother. Pharmacol.*, *59*, 397.
[12] Lai, Z., Yang, T., Kim, Y. B., Sielecki, T. M., Diamond, M. A. *et al.* (2002). *Proc. Natl. Acad. Sci. USA*, *99*, 14734.
[13] Konishi, Y., Hayase, F., & Kato, H. (1994). *Biosci. Biotech. Biochem.*, *58*, 1953.
[14] Hayase, F., Konishi, Y., & Kato, H. (1995). *Biosci. Biotech. Biochem.*, *59*, 1407.
[15] Sheldrick, G. M. (1997). SHELXS97, A Program for Automatic Solution of Crystal Structure. University of Göttingen: Germany.

[16] Sheldrick, G. M. (1997). *SHELX97, A Program for Crystal Structure Refinement*. University of Göttingen: Germany.
[17] Frisch, M. J., Trucks, G. W., Schlegel, H. B., Scuseria, G. E., Robb, M. A. *et al.* (2003). *Gaussian 03*, Gaussian, Inc., Pittsburgh PA.
[18] Asiri, A. M., Akkurt, M., Khanc, I. U., & Arshad, M. N. (2009). *Acta Cryst. E65*, o842.